nature genetics

Role of retrotransposon-derived imprinted gene, *Rtl1*, in the feto-maternal interface of mouse placenta

Yoichi Sekita[1], Hirotaka Wagatsuma[2], Kenji Nakamura[3], Ryuichi Ono[1], Masayo Kagami[4], Noriko Wakisaka[1,5], Toshiaki Hino[3], Rika Suzuki-Migishima[3], Takashi Kohda[1], Atsuo Ogura[6], Tsutomu Ogata[4], Minesuke Yokoyama[3,7], Tomoko Kaneko-Ishino[5] & Fumitoshi Ishino[1]

Eutherian placenta, an organ that emerged in the course of mammalian evolution, provides essential architecture, the so-called feto-maternal interface, for fetal development by exchanging nutrition, gas and waste between fetal and maternal blood. Functional defects of the placenta cause several developmental disorders, such as intrauterine growth retardation in humans and mice. A series of new inventions and/or adaptations must have been necessary to form and maintain eutherian chorioallantoic placenta, which consists of capillary endothelial cells and a surrounding trophoblast cell layer(s)[1]. Although many placental genes have been identified[2], it remains unknown how the feto-maternal interface is formed and maintained during development, and how this novel design evolved. Here we demonstrate that retrotransposon-derived *Rtl1* (retrotransposon-like 1), also known as *Peg11* (paternally expressed 11), is essential for maintenance of the fetal capillaries, and that both its loss and its overproduction cause late-fetal and/or neonatal lethality in mice.

To elucidate *Rtl1* function, we produced knockout (KO) mice (**Supplementary Fig. 1a**,**b** online). *Rtl1* is a paternally expressed imprinted gene highly expressed at the late-fetal stage in both the fetus and placenta (**Supplementary Fig. 1c**), and it is located in a large imprinted region on distal chromosome 12 (ref. 3; see **Supplementary Table 1** online for imprinting phenotypes[4–6]). Paternally expressed *Rtl1* has an overlapping maternally expressed antisense transcript, *Rtl1* antisense (*Rtl1as*, also known as *antiPeg11*), which contains several microRNAs (miRNAs) targeting the *Rtl1* transcript through an RNAi mechanism[3,7] (**Supplementary Fig. 1a**). We removed the entire Gag- and Pol-like domains of *Rtl1* with approximately 30% homology to the sushi-ichi retrotransposons, together with six of seven miRNAs in *Rtl1as*. Then, we produced two different types of mice: mice with no *Rtl1* expression upon paternal transmission of the KO allele (Pat-KO) and those with 2.5–3.0 times overexpression of the *Rtl1* as a result of deficiency of *Rtl1as* upon maternal transmission (Mat-KO; **Fig. 1a**). We confirmed that the imprinting regulation of distal chromosome 12 was not affected by the KO construct[8,9] (**Supplementary Fig. 1d**,**e**).

In the course of producing mice with the C57BL/6 (B6) background, we observed that the Pat-KO mice showed pre- and postnatal growth retardation in the F_1 and F_2 generations (**Supplementary Fig. 2a** online), and after the F_3 generation, most showed late-fetal or neonatal lethality (**Fig. 1b**,**c** and **Supplementary Fig. 3** online). When F_2 males mated with normal B6 females, all the pups, including the wild-type (WT) pups, were born dead as a result of a 3- to 4-d delay of the birth date (**Fig. 1c**; I and II in F_3 generation). When removed by caesarean sections at 19.0 days post coitus (d.p.c.) of the F_3 generation (**Fig. 1c**; III in F_3 generation), the WT pups grew normally, but half of the Pat-KO pups were already resorbing, and the other half were born small (about 80% the weight of the controls) and died by the next day (**Fig. 1c**; III in F_3 generation and **Table 1**). Pat-KO fetuses showed no abnormal phenotypes until 14.5 d.p.c., but half of them died from 15.5 to 19.0 d.p.c. (**Table 1**), and growth retardation of both the fetuses and placentas was observed even in the living half after 15.5 d.p.c. (**Fig. 1d–f**).

In Mat-KO mice, pups, at least after F_2, showed an approximately 15% retardation in growth after weaning (**Supplementary Fig. 2b**,**c**). Their birth rate gradually diminished after the F_4 generation, and neonatal lethality was predominant in the F_6 generation (**Fig. 1c**, F4–F6; **Supplementary Fig. 3b**, F_4–F_6 and **Supplementary Table 2** online). All the Mat-KO pups reached term normally, with normal weight, but they showed 150% placentomegaly compared to the normal size, and most died within a day (**Fig. 1g**,**h**). Although the genetic background affected both the Pat-KO and Mat-KO phenotypes to a large degree (**Supplementary Tables 2** and **3** online), these results demonstrate that both the loss and the overproduction

[1]Department of Epigenetics, Medical Research Institute, Tokyo Medical and Dental University, 2-3-10 Kandasurugadai, Chiyoda-ku, Tokyo 101-0062, Japan. [2]Graduate School of Bioscience and Biotechnology, Tokyo Institute of Technology, 4259 Nagatsuta-cho, Midori-ku, Yokohama 226-8501, Japan. [3]Mitsubishi Kagaku Institute of Life Sciences, 11 Minamiooya, Machida, Tokyo 194-8511, Japan. [4]Department of Endocrinology and Metabolism, National Research Institute for Child Health and Development, 2-10-1 Okura, Setagaya-ku, Tokyo 157-8535, Japan. [5]School of Health Sciences, Tokai University, Bohseidai, Isehara, Kanagawa 259-1193, Japan. [6]BioResource Center, RIKEN, 3-1-1 Koyadai, Tsukuba, Ibaraki 305-0074, Japan. [7]Present address: Brain Research Institute, Niigata University, 1-757 Asahimachi-dori, Niigata 951-8585, Japan. Correspondence should be addressed to T.K.-I. (tkanekoi@is.icc.u-tokai.ac.jp) or F.I. (fishino.epgn@mri.tmd.ac.jp).

Received 21 May 2007; accepted 16 October 2007; published online 6 January 2008; doi:10.1038/ng.2007.51

of *Rtl1* interfered with normal fetal development, providing direct evidence for the importance of both retrotransposon-derived *Rtl1* and microRNAs in *Rtl1as*.

Histological analyses demonstrated that severe abnormalities occur in the same place in both the Pat-KO and Mat-KO placentas (that is, the fetal capillaries where the feto-maternal interaction occurs), but the consequences of these abnormalities were different (**Fig. 2**). The mouse placenta consists of three major zones: the decidua basalis, the junctional zone and the labyrinth zone. In the Pat-KO placenta at 15.5 d.p.c., we found abnormal, dark-stained regions in the labyrinth zone upon hematoxylin and eosin (HE) staining (**Fig. 2a**, WT; **b**,**c**, Pat-KO). Using truidin blue staining and electron microscopy, we confirmed several morphological abnormalities throughout the labyrinth zone, such as splitting of the basement membrane (**Fig. 2d**,**h**, WT; **e**,**i**, Pat-KO), the emergence of a number of lysosomes in layer III trophoblast cells (**Fig. 2f**,**j**) and clogging in the fetal capillaries (**Fig. 2g**,**k**). When we did immunohistochemical (IHC) staining with CD31, an endothelial cell–specific marker, we observed that its

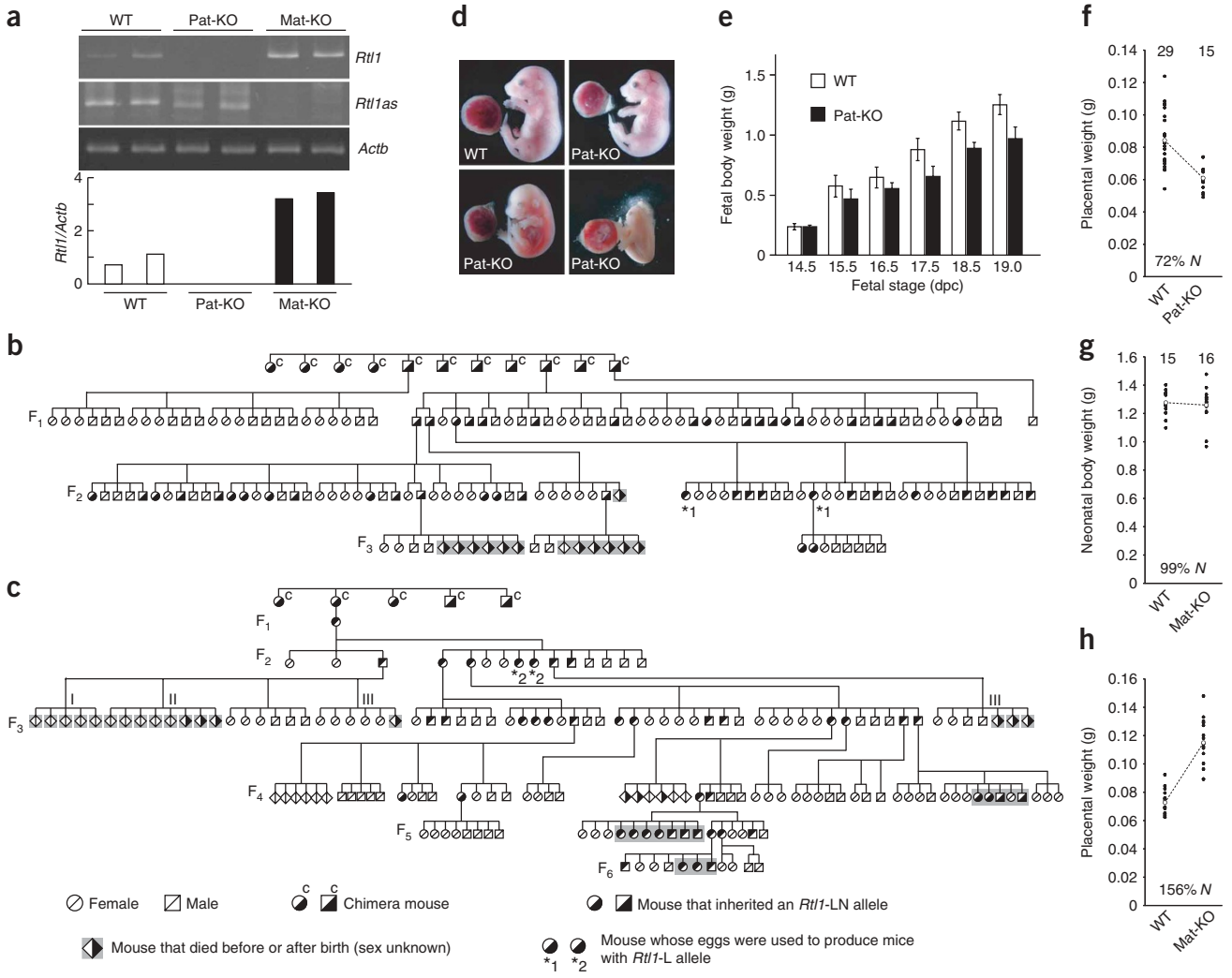

Figure 1 Pedigree of *Rtl1* KO mice. (**a**) Expression of *Rtl1* and *Rtl1as* in WT, Pat-KO and Mat-KO fetuses (*Rtl1*-LN) as determined by RT-PCR. β-actin (encoded by *Actb*) used as a control. The band intensities, measured using ImageJ software are shown below. (**b**) A pedigree from a male chimera. (**c**) A pedigree from a female chimera. A 4-d delay of natural delivery (I) and a caesarean section after a 3-d delay from the expected delivery date (II). All pups were dead in both cases. Caesarean sections were carried out at 19.0 d.p.c. when paternal transmission was analyzed (III). From the F_1 males and females, we obtained many Pat-KO and Mat-KO mice, although the number of Pat-KO mice was slightly smaller than expected from the mendelian ratio (WT/Pat-KO = 24:19, **Supplementary Table 1**) and they grew to adulthood with a reduced body weight (**Supplementary Fig. 2**). Thus, it is clear that the F_1 males and females with the C57BL/6 × 129/Sv F1 (B6/129) genetic background from chimera mice can produce some viable Pat-KO and Mat-KO pups. (**d**) Fetuses at 16.5 d.p.c, including a WT fetus (upper left) and Pat-KO fetuses: small normal-looking (alive) fetus (upper right), pale dead fetus (lower left), and resorbing fetus (lower right). Scale bar, 10 mm. (**e**) Late-fetal growth retardation in Pat-KO fetuses. Open bars, WT fetal body weight; solid bars, Pat-KO fetal body weight. (**f–h**) Growth phenotype of Pat-KO placentas at 18.5 d.p.c. (**f**) and Mat-KO neonates (**g**) and Mat-KO placentas (**h**) at birth (caesarean section). The data in **g** and **h** are from the same litters. Each filled circle represents a single placenta and neonate, respectively. The number at the top represents the total number of weighted samples. Open circles represent average weight. The degree of growth deficiency or promotion of mutant mice is shown as the percentage of WT weight (*N*). Placental and neonatal body weights (mean ± s.d.) are as follows: **f**; WT, 0.085 ± 0.015 ($n = 29$); Pat-KO, 0.061 ± 0.008 ($n = 15$); $P = 1.805 \times 10^{-65}$ (*t*-test), **g**; WT, 1.279 ± 0.087 ($n = 15$); Mat-KO, 1.262 ± 0.126 ($n = 16$), **h**; WT, 0.073 ± 0.009 ($n = 15$); Mat-KO, 0.116 ± 0.016 ($n = 16$); $P = 9.721 \times 10^{-105}$ (*t*-test).

Table 1 Lethality of *Rtl1*-LN (Pat-KO) fetuses and neonates at F_3

Dissection stage (d.p.c.)	WT total	Pat-KO total (dead)	Percentage death in Pat-KO
12.5	5	4 (0)	0
14.5	5	5 (0)	0
15.5	9	7 (1)	14.3
16.5	9	11 (5)	45.5
17.5	10	11 (6)	54.5
18.5	21	24 (13)	54.2
Neonate	35	13 (13)	100

signal diffused to the area of the trophoblast cells (**Fig. 2l**, WT; **m**,**n**, Pat-KO). These results indicate that a phagocytic reaction to the endothelial cells was induced in the surrounding layer III trophoblast cells. Thus, the resulting placental infarction seems to cause placental malfunction, such as incomplete material transport between the maternal and the fetal blood, presumably leading to the late-fetal growth retardation and lethality in the Pat-KO fetuses.

We confirmed functional deficiency of the Pat-KO placenta by nutrition transfer assay[10,11]. We examined both active and passive transport at 15.5 d.p.c. using two radiolabeled substrates, [^{14}C]methylaminoisobutyric acid (Me-AIB) and [^{14}C]inulin, respectively. We did not find any significant difference between WT and Pat-KO placentas in materno-fetal transfer of [^{14}C]Me-AIB, a non-metabolizable amino acid analog, through the System A amino acid transport system ($P = 0.158$; **Fig. 3a**). However, the passive permeability of inulin was significantly lower in Pat-KO placenta (48% compared with WT, $P = 0.000123$; **Fig. 3b**), indicating that Rtl1 deficiency had damaged the placental physical barrier but had not affected the active transport system[12]. In the case of Mat-KO, placentomegaly was associated with expansion of the inner spaces of the fetal capillaries (**Fig. 1h** and **Fig. 2o**, WT; **p**, Mat-KO, and **q**). The most severe abnormalities were found in the surrounding layer III trophoblast cells, which showed a large number of vacuoles, indicating that these cells were starving (**Fig. 2r**, WT; **s**,**t**, Mat-KO).

IHC staining with antibody to Rtl1 showed that Rtl1 protein localized exclusively in the labyrinth zone at 18.5 d.p.c.; no signals in the other layers of the placenta were observed (**Fig. 4a–d**). Co-immunostaining with CD31 showed that Rtl1 localized around the nuclei of the capillary endothelial cells, where anomalies in both Pat-KO and Mat-KO were observed (**Fig. 4e**). We did not observe any signals in the Pat-KO placentas, but we observed strong signals in the

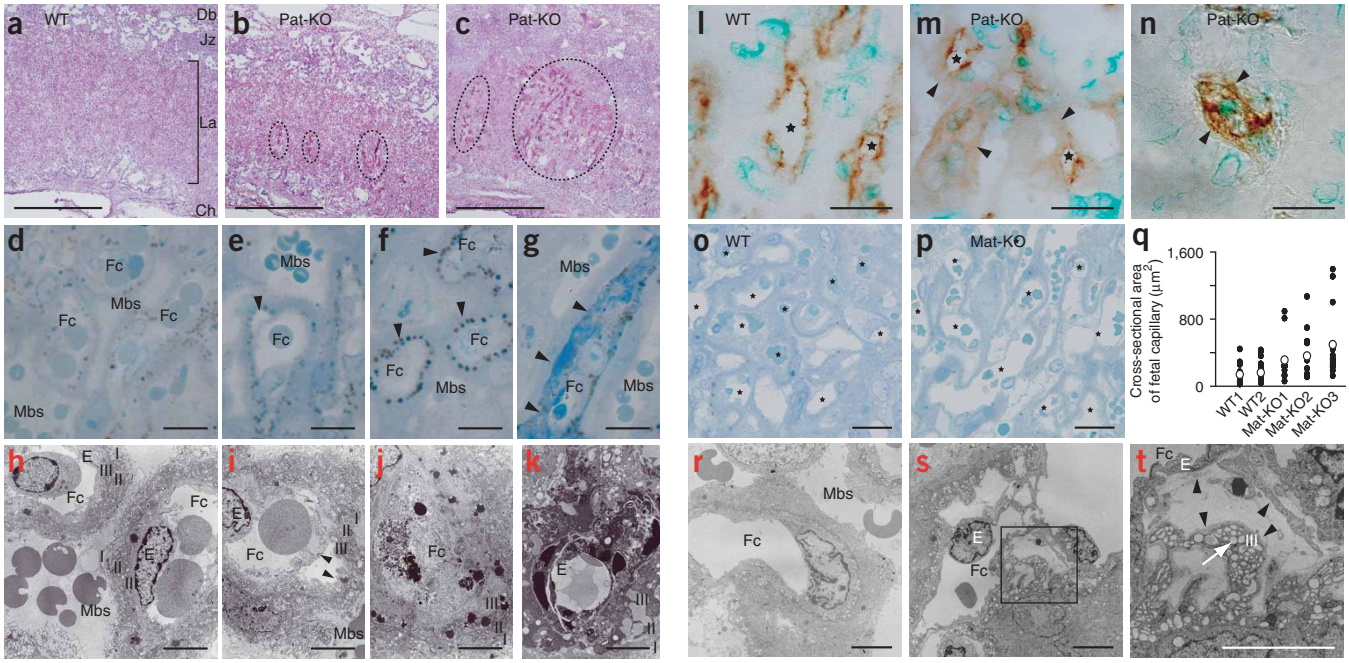

Figure 2 Histological abnormalities observed in day 15.5 Pat-KO placentas and in day 18.5 Mat-KO placentas. Most abnormalities were observed near the endothelial cells and the surrounding layer III trophoblast of the fetal capillaries in the labyrinth zone. (**a**–**n**) The labyrinth zone of WT placentas at 15.5 d.p.c. is shown in **a**, **d**, **h** and **l** and that of Pat-KO placentas at the same stage is shown in **b**, **c**, **e**–**g**, **i**–**k**, **m** and **n**. (**o**–**s**) The labyrinth zone of WT placenta at 18.5 d.p.c. is shown in **o** and **r**, and that of the Mat-KO placenta at the same stage is shown in **p** and **s**. H&E staining in **a**–**c**; scale bar, 0.5 mm. Truidin blue staining in **d**–**g**,**o** and **p**; scale bar, 10 μm for **d**–**g**, 20 μm for **o** and **p**. The arrowheads indicate an abnormal space between the endothelial cell and the layer III trophoblast in **e**, abnormally appearing lysosomes in **f** and a clogged fetal capillary in **g**. Clogging, as seen in **g** and **k**, was found mainly in the dark-stained regions, as shown in the dotted circles in **b** and **c**. Electron microscopy images in **h**–**k**,**r** and **s**; scale bar, 5 μm. The arrowheads indicate an abnormal space between the endothelial cell and the layer III trophoblast in **i**. (**t**) Magnified figure of the square area in **s**; scale bar, 5 μm. The black arrowheads indicate an abnormal space between the endothelial cell and the layer III trophoblast, and the white arrow indicates vacuoles in the layer III trophoblast. IHC staining in **l**–**n** with antibody to CD31; scale bar, 20 μm. The arrowheads indicate an abnormally diffused signal of endothelial cell marker in **m** and a disrupted fetal capillary in **n**. The same result was obtained with an antibody to CD34, another endothelial specific marker (data not shown). **q** shows a cross-sectional area of fetal capillary that was measured using ImageJ. The Pat-KO fetus associated with placenta **c** and **n** was already dead at 15.5 d.p.c. At present, it remains unclear whether the neonatal lethal phenotypes in both Pat-KO and Mat-KO are primarily due to direct or indirect effects of the severe placental anomalies, although both are likely to be involved. Further investigation will be necessary to reveal whether there is a specific cause for neonatal lethality. Db, decidua basalis; Jz, junctional zone; Lz, labyrinth zone; Ch, chorionic plate; Mbs, maternal blood sinus; Fc, fetal capillary; E, endothelial cell; I/II/III, layer I/II/III trophoblast. The asterisks in **l**–**p** indicate fetal capillaries.

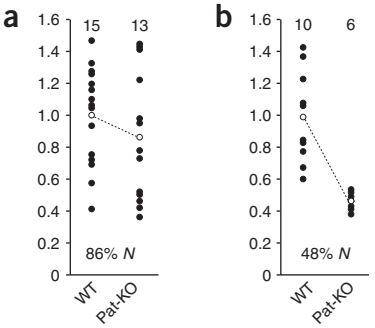

Figure 3 Placental transfer assay. (**a**) Placental transfer of [^{14}C]Me-AIB at 15.5 d.p.c. (**b**) Placental transfer of [^{14}C]inulin at 15.5 d.p.c. Each substrate was injected from the jugular vein of pregnant females at 15.5 d.p.c., and the amount of the labeled substances that entered the fetus through the placenta was determined 3–4 min after injection[10,11]. The fetal accumulation of radioisotope per milligram of placenta was calculated and compared between WT and Pat-KO. The average of WT in every littermate was defined as 1. No significant difference in the active transfer of Me-AIB between WT and Pat-KO placenta was found (86%, $P = 0.158$). However, the passive permeability of inulin in Pat-KO was decreased to about 50% of that in WT (48%, $P = 0.000123$).

Mat-KO placentas, as expected (**Fig. 4f,g**; see also **Supplementary Fig. 4** online). No Rtl1 protein was detected in the endothelial cells of the umbilical cord, although they are connected to the fetal capillaries and are of the same origin as placental endothelial cells (**Fig. 4a,d**). Therefore, we concluded that Rtl1 functions exclusively in the placental endothelial cells for the maintenance of the feto-maternal interface during late-fetal development. To create the novel feto-maternal interface in the course of evolution, the endothelial cells may need a unique protein to regulate the trophoblast cells that have intrinsically invasive and phagocytotic features.

These experiments demonstrate that among several candidate imprinted genes, *Rtl1* is one of the major genes responsible for maternal and paternal duplication of distal chromosome 12 (PatDp (dist12) and MatDp(dist12)) as well as for the corresponding uniparental disomies (MatDi(12) and PatDi(12))[4–6] (**Supplementary Table 1**). The MatDp(dist12) phenotypes of late-fetal and neonatal lethality associated with intrauterine growth retardation are consistent with those of *Rtl1* Pat-KO. *Dlk1* Pat-KO and *Dio3* null mice also showed reduced neonatal size and viability to a certain degree, but this did not account for the severe lethality of MatDp(dist12) and MatDi(12)[13,14]. Therefore, we conclude that the loss of *Rtl1* expression has an important role in such late-fetal viability and that *Dlk1, Rtl1* and possibly *Dio3* can independently contribute to late-fetal growth and neonatal lethality. *Rtl1* Mat-KO mice show notable overgrowth and morphological abnormalities of the placenta consistent with the PatDi(12) mice phenotypes[15]. The Mat-KO mice show only a 2.5- to 3.0-fold increment of *Rtl1* from a single normal paternal allele as a result of the lack of *Rtl1as* from the maternal allele. Therefore, an approximately 4.5-fold overexpression of *Rtl1* from the two paternal alleles that would be expected in PatDi(12) and PatDp(dist12) mice[9] may explain their late-fetal lethality, rather than the neonatal lethality in the Mat-KO.

Rtl1 is one of 11 retrotransposon-derived genes related to the sushi-ichi retrotransposon that are specifically conserved in eutherian mammals[16–20]. Eutherian orthologs of *Rtl1* have a high degree of amino acid conservation and low synonymous-to-nonsynonymous substitution rates (dN/dS), supporting the claim that *Rtl1* has a common and crucially important function in the placenta among eutherians, including human beings[17,21] (**Supplementary Fig. 5** online). This work provides evidence for exaptation, the acquisition

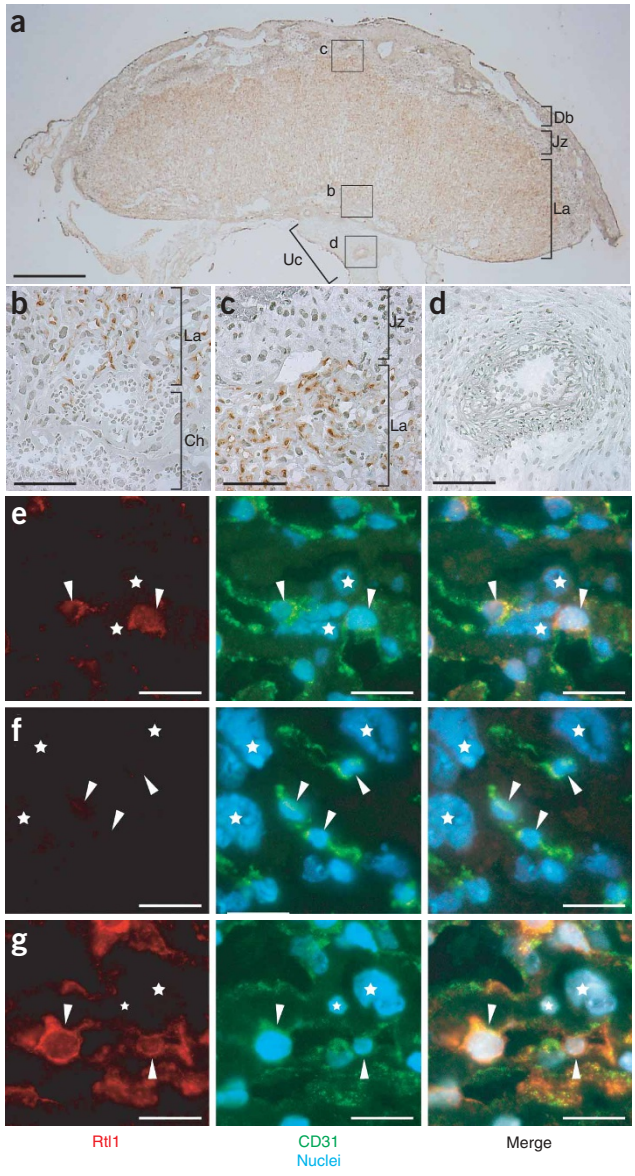

Figure 4 Rtl1 protein localization in the placentas at 18.5 d.p.c. by immunohistochemistry. (**a**–**c**) Whole placenta image (**a**) and its magnified images (indicated as each small square) of the boundary regions of the placental zones between the labyrinth zone (La) and chorionic plate (Ch) (**b**) and between La and the junctional zone (Jz) (**c**). (**d**) Umbilical cord (Uc) connecting to the fetal capillaries. The signals of Rtl1 (brown by DAB staining) are seen exclusively in La but not in Ch, Jz, decidual basalis (Db) or Uc. Scale bar, 1 mm for **a** and 100 μm for **b**–**d**. (**e**–**g**) Co-immunostaining of Rtl1 (red, left), CD31 and nuclei (green and blue, respectively, middle) and their merged image (right). The labyrinth zones of WT (**e**), Pat-KO (**f**) and Mat-KO (**g**) are shown. The arrowheads and stars indicate nuclei of endothelial cells and trophoblast cells, respectively. Scale bar, 20 μm. Only the perinuclear region in the endothelial cells were stained by antibody to Rtl1 in WT (**e**) and Mat-KO (**g**). Note that the inner areas of the endothelial cells were also stained when Rtl1 was overproduced in Mat-KO (**g**; left and right).

of new genomic function from transposons[22–29]. We have recently shown that *Peg10* is also essential for placenta formation[18]. Although both *Rtl1* and *Peg10* are derived from the sushi-ichi–related retrotransposon, they have divergent roles, as expected from their amino acid sequences and as shown by the results of knockout experiments. *Peg10* has a DNA/RNA binding motif and an aspartyl protease motif, and it functions in placenta formation, especially in the trophoblast lineage, at an early embryonic stage. *Rtl1*, however, has only an aspartyl protease motif and functions in the maintenance of the feto-maternal interface at the late-fetal stage[16]. The important implication of these findings is that two independent exaptation events of the sushi-ichi–related retrotransposons have contributed to two different steps of placental development in the mouse.

In this work, we demonstrate that the retrotransposon-derived gene *Rtl1* is a key gene in placental development and evolution and is one of the primary genes responsible for phenotypic development in mouse PatDp(dist12)/MatDp(dist12) as well as PatDi(12)/MatDi(12). Because the remaining nine retrotransposon-derived genes also possess putative proteins, and at least some of them show expression in the placenta[16–20], identification of their origins and functions may provide important insight into placental evolution.

METHODS

Deletion of the *Rtl1* gene. Experimental procedures in this work were approved by the Animal Ethics Committees of Tokyo Medical and Dental University. We obtained 1.8-kb (nucleotides 67,582,103–67,580,338) and 7.3-kb (nucleotides 67,586,373–67,593,715) genomic DNA fragments from a mouse BAC (mRG158M19) clone containing the *Rtl1* ORF (nucleotides 67,581,614–67,586,845) and used them as the right- and left-arm sequences of a construct in which the *Rtl1* ORF was replaced with the neomycin-resistance gene. The nucleotide numbers refer to the sequence with accession number NT_039551.6. After a 2-week incubation under G418 selection, followed by electroporation of the linearized DNA into embryonic stem cells (CCE) of 129/SvEv mouse origin, we obtained 120 colonies. The genomic DNA was checked using DNA blot analysis with DNA fragments of nucleotides 67,580,998–67,581,906 and 67,607,241–67,608,065 as the 5′ and 3′ probes, respectively.

Using the *Rtl1*-targeted embryonic stem cells resulting from the homologous recombination of the construct, we made chimeric mice by blastocyst injection. Germline transmission of the knockout allele was confirmed in one male and one female chimera (*Rtl1*-LN). We carried out *in vitro* fertilization using normal C57BL/6 sperm and eggs from two *Rtl1*-LN females (indicated by the asterisks 1 and 2 in **Figure 1b** and **c**, respectively) and injected the *Cre* recombinase expression vector (pCAGGS-Cre) into the resulting fertilized eggs to produce mice that had *Rtl1*-L alleles.

All of the *Rtl1* KO lines were maintained by continuous crossing with WT B6 males and females to the F_8 generation, unless otherwise indicated.

Expression analyses of imprinted genes. Genomic DNA and total RNA were prepared from day 14.5 fetuses using ISOGEN (Nippon Gene). The methods for the quantitative RT-PCR for *Dlk1*, *Dio3*, *Meg3/Gtl2*, *Meg8/Rian* and 3′-RACE for *Rtl1* and *Rtl1as* followed by cDNA synthesis have been described previously[30]. The band intensity of *Rtl1* was measured using ImageJ software (see URLs section below).

DNA methylation analyses of IG-DMR and *Gtl2*-DMR. Purified genomic DNA was treated with sodium bisulfite solution, and the resulting DNA was amplified by the primers described previously[30]. We used the combined bisulfite restriction analysis (COBRA) method with the restriction enzyme *Aci*I for IG-DMR and *Taq*I for *Gtl2*-DMR.

Placenta functional assay. We examined the efficiencies of nutrition transfer through the placenta at 15.5 d.p.c. in every fetus and placenta of the two to three litters using two radiolabeled substrates, [^{14}C]Me-AIB and [^{14}C]inulin, to measure the active and passive transport, respectively[10,11]. These substrates were dissolved in PBS and injected into the jugular vein of pregnant females. Three to four minutes after injection, the females were dissected and fetuses and placentas were sampled, because it is reported that there is minimal backflux of the radioisotopes from fetus to mother for up to 5 min[11]. The amount of the labeled substance in the fetuses and placentas was determined by a liquid scintillation counter. The counts of fetuses per milligram of placentas were calculated as the placental transfer efficiency, and the average of WT fetuses in each litter was set as 1. We compared WT and Pat-KO. Materno-fetal transfer of Me-AIB, a non-metabolizable amino acid analog usually transported across the placenta, reflects the activity of the System A amino acid transport system, whereas that of inulin reflects the passive permeability that is usually affected by the exchange barrier surface area, thickness and fetal blood flow. Using this assay, we detected only background levels of radioisotopes in the dead fetuses, whereas we found that the levels in their placentas were almost the same as that of WT and living Pat-KO placentas, providing evidence that the maternal blood flow in the placentas was still normal, even in the dead fetuses.

Histological analyses. The placentas for hematoxylin and eosin staining and IHC staining were collected and embedded in OCT compound immediately. Then, 5-μm sections were made. For hematoxylin and eosin staining, we fixed the sections in 4% paraformaldehyde (PFA) before performing the standard staining procedure. The sections were fixed in acetone for the immunostaining of CD31 and CD34, or 4% PFA for the immunostaining of Rtl1. Antibody to CD31 and antibody to CD34 (BD Pharmingen) were each used as the primary antibody, and then horseradish peroxidase (HRP)-labeled anti-rat IgG (Jackson ImmunoResearch Laboratories) was added as the secondary antibody. The antibody to Rtl1 that was produced from rabbit serum by immunizing with the synthetic Rtl1 peptide (NH_2-CGDQEAVTFRPRN-COOH) was used as the primary antibody, and then HRP-labeled anti-rabbit IgG (GE Healthcare Bio-Sciences) was added as the secondary antibody. HRP activities were visualized by diaminobenzidine (DAB) staining, and the nuclei were stained using 2% methyl green. For co-immunostaining of Rtl1 and CD31, the sections were fixed in 4% PFA. The primary antibody mixture including the antibody to CD31 and the antibody to Rtl1, and the secondary antibody mixture including the Alexa 488-conjugated anti-rat IgG (Invitrogen), Cy3-conjugated anti-rabbit IgG (Jackson ImmunoResearch Laboratories) and Hoechst 33342, were used. Images were captured and overlaid by a VB-7000 Digital Camera System (Keyence). For truidin blue staining and transmission electron microscopy, we fixed the placentas in 2.5% glutaraldehyde in 0.05 M PBS and 1% osmium tetroxide before following the standard staining methodology.

URLs. ImageJ software, http://rsb.info.nih.gov/ij/.

GenBank accession codes. The nucleotide numbers refer to the sequence of mouse chromosome 12 with accession number NT_039551.6.

Note: Supplementary information is available on the Nature Genetics website.

ACKNOWLEDGMENTS

We thank S. Aizawa of Center for Developmental Biology, RIKEN for providing the DT-A vector that was used for making *Rtl1* KO construct, E. Robertson of University of Oxford for the CCE ES cells, M. Constancia of University of Cambridge for placenta functional assay protocol, Y. Nakahara and M. Takabe of the Mitsubishi Kagaku Institute of Life Sciences for animal breeding and H. Hasegawa, N. Kawabe and A. Akatsuka of the Tokai University and S. Ichinose of the Tokyo Medical and Dental University for their assistance in immunohistochemistry and electron microscopy along with helpful discussion. This work was supported by grants from Creative Science Research, the research program of Japan Society for the Promotion of Science (JSPS), the Uehara Memorial Science Foundation, the Mitsubishi Foundation and the Ministry of Health, Labour and Welfare for Child Health and Development (17C-2) and a Grant-in-Aid for Scientific Research on Priority Areas form the Ministry of Education, Culture, Sports, Science and Technology of Japan (1508023) to F.I., the grant for young investigators from Medical Research Institute to Y.S., and the Asahi Glass Foundation and JSPS, Grants-in Aid for Scientific Research to T.K.-I. Pacific Edit reviewed the manuscript before submission.

AUTHOR CONTRIBUTIONS

Most analyses in this work were performed by Y.S. with collaboration of H.W., R.O., N.W., T.K. and M.K. in molecular and histological experiments.

Construction of *Rtl1* targeting vector was done by H.W. under supervision of K.N. and M.Y., and KO mice were produced by T.H., R.S.-M., K.N. and M.Y. The study was designed and coordinated by T.K.-I. and F.I., and the results were discussed by A.O., T.O., T.K.-I. and F.I. The paper was written by Y.S. and F.I.

Published online at http://www.nature.com/naturegenetics
Reprints and permissions information is available online at http://npg.nature.com/reprintsandpermissions

1. Rossant, J. & Cross, J.C. Placental development: lessons from mouse mutants. *Nat. Rev. Genet.* **2**, 538–548 (2001).
2. Watson, E.D. & Cross, J.C. Development of structures and transport functions in the mouse placenta. *Physiology (Bethesda)* **20**, 180–193 (2005).
3. Seitz, H. *et al.* Imprinted microRNA genes transcribed antisense to a reciprocally imprinted retrotransposon-like gene. *Nat. Genet.* **34**, 261–262 (2003).
4. Cattanach, B.M. & Rasverry, C.V. Evidence of imprinting involving the distal region of Chr 12. *Mouse Genome* **91**, 858 (1993).
5. Georgiades, P., Watkins, M., Surani, M.A. & Ferguson-Smith, A.C. Parental origin-specific developmental defects in mice with uniparental disomy for chromosome 12. *Development* **127**, 4719–4728 (2000).
6. Tevendale, M., Watkins, M., Rasberry, C., Cattanach, B. & Ferguson-Smith, A.C. Analysis of mouse conceptuses with uniparental duplication/deficiency for distal chromosome 12: comparison with chromosome 12 uniparental disomy and implications for genomic imprinting. *Cytogenet. Genome Res.* **113**, 215–222 (2006).
7. Davis, E. *et al.* RNAi-mediated allelic trans-interaction at the imprinted *Rtl1/Peg11* locus. *Curr. Biol.* **15**, 743–749 (2005).
8. Takada, S. *et al.* Epigenetic analysis of the *Dlk1-Gtl2* imprinted domain on mouse chromosome 12: implications for imprinting control from comparison with *Igf2-H19*. *Hum. Mol. Genet.* **11**, 77–86 (2002).
9. Lin, S.P. *et al.* Asymmetric regulation of imprinting on the maternal and paternal chromosomes at the *Dlk1-Gtl2* imprinted cluster on mouse chromosome 12. *Nat. Genet.* **35**, 97–102 (2003).
10. Constância, M. *et al.* Placental-specific IGF-II is a major modulator of placental and fetal growth. *Nature* **417**, 945–948 (2002).
11. Sibley, C.P. *et al.* Placental-specific insulin-like growth factor 2 (*Igf2*) regulates the diffusional exchange characteristics of the mouse placenta. *Proc. Natl. Acad. Sci. USA* **101**, 8204–8208 (2004).
12. Angiolini, E. *et al.* Regulation of placental efficiency for nutrient transport by imprinted genes. *Placenta* **27** (Suppl. A), S98–S102 (2006).
13. Moon, Y.S. *et al.* Mice lacking paternally expressed Pref-1/Dlk1 display growth retardation and accelerated adiposity. *Mol. Cell. Biol.* **22**, 5585–5592 (2002).
14. Hernandez, A., Martinez, M.E., Fiering, S., Galton, V.A. & St Germain, D. Type 3 deiodinase is critical for the maturation and function of the thyroid axis. *J. Clin. Invest.* **116**, 476–484 (2006).
15. Georgiades, P., Watkins, M., Burton, G.J. & Ferguson-Smith, A.C. Roles for genomic imprinting and the zygotic genome in placental development. *Proc. Natl. Acad. Sci. USA* **98**, 4522–4527 (2001).
16. Butler, M., Goodwin, T., Simpson, M., Singh, M. & Poulter, R. Vertebrate LTR retrotransposons of the Tf1/sushi group. *J. Mol. Evol.* **52**, 260–274 (2001).
17. Lynch, C. & Tristem, M. A co-opted gypsy-type LTR-retrotransposon is conserved in the genomes of humans, sheep, mice, and rats. *Curr. Biol.* **13**, 1518–1523 (2003).
18. Ono, R. *et al.* Deletion of *Peg10*, an imprinted gene acquired from a retrotransposon, causes early embryonic lethality. *Nat. Genet.* **38**, 101–106 (2006).
19. Brandt, J. *et al.* Transposable elements as a source of genetic innovation: expression and evolution of a family of retrotransposon-derived neogenes in mammals. *Gene* **345**, 101–111 (2005).
20. Youngson, N.A., Kocialkowski, S., Peel, N. & Ferguson-Smith, A.C. A small family of sushi-class retrotransposon-derived genes in mammals and their relation to genomic imprinting. *J. Mol. Evol.* **61**, 481–490 (2005).
21. Kagami, M. *et al.* Deletions and epimutations affecting the human 14q32.2 imprinted region in individuals with paternal and maternal upd(14)-like phenotypes. *Nat. Genet.* advance online publication, doi:10.1038/ng.2007.56 (6 January 2008).
22. Gould, S. & Vrba, S. Exaptation—a missing term in the science of form. *Paleobiology* **8**, 4–15 (1982).
23. Brosius, J. & Gould, S.J. On "genomenclature": a comprehensive (and respectful) taxonomy for pseudogenes and other "junk DNA". *Proc. Natl. Acad. Sci. USA* **89**, 10706–10710 (1992).
24. Smit, A.F. Interspersed repeats and other mementos of transposable elements in mammalian genomes. *Curr. Opin. Genet. Dev.* **9**, 657–663 (1999).
25. Mi, S. *et al.* Syncytin is a captive retroviral envelope protein involved in human placental morphogenesis. *Nature* **403**, 785–789 (2000).
26. Kazazian, H.H., Jr. Mobile elements: drivers of genome evolution. *Science* **303**, 1626–1632 (2004).
27. Dupressoir, A. *et al.* Syncytin-A and syncytin-B, two fusogenic placenta-specific murine envelope genes of retroviral origin conserved in Muridae. *Proc. Natl. Acad. Sci. USA* **102**, 725–730 (2005).
28. Bejerano, G. *et al.* A distal enhancer and an ultraconserved exon are derived from a novel retroposon. *Nature* **441**, 87–90 (2006).
29. Biémont, C. & Vieira, C. Genetics: junk DNA as an evolutionary force. *Nature* **443**, 521–524 (2006).
30. Sekita, Y. *et al.* Aberrant regulation of imprinted gene expression in *Gtl2*^{lacZ} mice. *Cytogenet. Genome Res.* **113**, 223–229 (2006).